



# sox2 and sox3 cooperate to regulate otic/epibranchial placode induction in zebrafish



Yunzi Gou, Jinbai Guo, Kirstin Maulding, Bruce B. Riley\*

Department of Biology, Texas A & M University, College Station, TX 77843-3258, United States

## ARTICLE INFO

### Keywords:

SoxB1  
Pluripotency  
Progenitors  
TALEN  
CRISPR/Cas9

## ABSTRACT

Expression of *sox3* is one of the earliest markers of Fgf-dependent otic/epibranchial placode induction. We report here that *sox2* is also expressed in the early otic/epibranchial placode in zebrafish. To address functions of *sox2* and *sox3*, we generated knockouts and heat shock-inducible transgenes. Mutant analysis, and low-level misexpression, showed that *sox2* and *sox3* act redundantly to establish a full complement of otic/epibranchial cells. Disruption of *pax8*, another early regulator, caused similar placodal deficiencies to *sox3* mutants or *pax8-sox3* double mutants, suggesting that *sox3* and *pax8* operate in the same pathway. High-level misexpression of *sox2* or *sox3* during early stages cell-autonomously blocked placode induction, whereas misexpression several hours later could not reverse placodal differentiation. In an assay for ectopic placode-induction, we previously showed that misexpression of *fgf8* induces a high level of ectopic *sox3*, but not *pax8*. Partial knockdown of *sox3* significantly enhanced ectopic induction of *pax8*, whereas full knockdown of *sox3* inhibited this process. Together these findings show that *sox2* and *sox3* are together required for proper otic induction, but the level of expression must be tightly regulated to avoid suppression of differentiation and maintenance of pluripotency.

## 1. Introduction

The otic placode, the precursor of the inner ear, is induced by Fgfs emanating from the hindbrain and subjacent mesendoderm during a period lasting from late gastrulation through early segmentation (Alvarez et al., 2003; Freter et al., 2008; Léger and Brand, 2002; Ladher et al., 2005; Liu et al., 2003; Mansour et al., 1993; Maroon et al., 2002; Martin and Groves, 2006; Maulding et al., 2014; Padanad et al., 2012; Park and Saint-Jeannet, 2008; Wright and Mansour, 2003). After a brief lag, epibranchial placodes are also induced by Fgf and share many of the same early markers. In zebrafish, *pax8* and *sox3* are the earliest markers of otic and epibranchial development (Nikaido et al., 2007; Phillips et al., 2001; Sun et al., 2007). Loss-of-function and overexpression studies show that *pax8* helps initiate otic differentiation and, together with *pax2a* and *pax2b*, maintains otic fate as the placode gives rise to the otic vesicle (Hans et al., 2004; Ikenaga et al., 2011; Mackereth et al., 2005; Padanad et al., 2012). Loss of *pax2/8* function does not block epibranchial placode formation (Mackereth et al., 2005) but does impair subsequent differentiation of epibranchial ganglia (Padanad and Riley, 2011). The role of *sox3* in otic/epibranchial development is less well defined and has heretofore been examined primarily using morpholino oligomer (MO)-mediated gene knockdown (Padanad and Riley, 2011). Knockdown of either *sox3* or *pax8* causes

moderate reduction in the size of the otic placode, whereas knockdown of both *sox3* and *pax8* causes a more severe reduction. Similarly, knockdown of *sox3* causes partial loss of epibranchial ganglia and simultaneous knockdown of *pax8* strongly enhances this phenotype. These data suggest that *pax8* and *sox3* each provide some non-overlapping functions required for early otic differentiation. However, concerns over possible off-target effects of MOs highlight the need to analyze gene knockouts in order to corroborate or refine previous findings (Kok et al., 2015; Rossi et al., 2015; Schulte-Merker and Stainier, 2014).

Expression of *sox3* is regulated in a dynamic fashion by changing levels of Fgf. Initially *sox3* is induced at a relatively high level in otic cells in the early response to Fgf (Nikaido et al., 2007; Sun et al., 2007). Subsequently, *sox3* expression declines to a discrete lower level in the otic placode in response to locally rising Fgf levels (Bhat and Riley, 2011; Maulding et al., 2014; Padanad and Riley, 2011). At the same time *sox3* is induced at a relatively high level in prospective epibranchial cells abutting the lateral edge of the otic placode. The significance of reducing *sox3* expression in the otic placode is not known but potentially reflects a requirement for developmental progression. Sox3 is a member of the SoxB1 family of transcription factors, which are known to maintain pluripotency of progenitors or promote early stages of differentiation, depending on the level of expression (Gómez-López

\* Corresponding author.

E-mail address: [briley@mail.bio.tamu.edu](mailto:briley@mail.bio.tamu.edu) (B.B. Riley).

et al., 2011; Hutton and Pevny, 2011; Juuri et al., 2012; Kondoh and Kamachi, 2010; Matsushima et al., 2011; Packard et al., 2016; Rizzino and Wuebben, 2016; Tucker et al., 2010). Accordingly, dynamic regulation of *sox3* might modulate the balance of pluripotency vs. differentiation during early otic development.

Another variable that could influence *sox3* function is overlapping expression of the related gene *sox2*. We previously reported that otic expression of *sox2* begins at 14 hpf (10 somite stage) in association with early development of sensory epithelia (Millimaki et al., 2010). However, we recently discovered that low-level expression of *sox2* can be detected in the otic/epibranchial region as early as 12–12.5 hpf (6 somite stage). This raises the possibility that *sox2* provides some degree of redundancy with *sox3* during otic/epibranchial placode induction, and it could also affect the balance of pluripotency vs. differentiation by elevating overall SoxB1 levels.

To address the above issues, we generated knockout lines and heat shock-inducible transgenic lines for *sox2* and *sox3* to evaluate their functions in otic and epibranchial placode development. Knockouts of *sox2* and *sox3* cause phenotypes that closely mimic their respective MO phenotypes. Mutant analysis confirms that *sox2* and *sox3* provide partially redundant functions required for establishing a normal amount of otic and epibranchial tissue. Weak misexpression of *sox2* can rescue placodal deficiencies caused by loss of *sox3*, consistent with functional redundancy. However, strong misexpression of either *sox2* or *sox3* cell-autonomously blocks initial stages of otic differentiation, confirming that the function of these genes is concentration-dependent. We also confirm that *pax8*<sup>-/-</sup> mutants (like *pax8*-morphants) show a more severe placodal deficiency than *sox3*<sup>-/-</sup> mutants, but the placodal deficiency is no worse in *pax8*<sup>-/-</sup>; *sox3*<sup>-/-</sup> double mutants. This suggests that *pax8* and *sox3* work together in the same pathway rather than providing distinct gene-specific functions.

## 2. Materials and methods

### 2.1. Fish strains and developmental conditions

The wild-type strain was derived from the AB line (Eugene, OR). The *pax2a* mutant allele *noi<sup>tu29a</sup>* (Brand et al., 1996; Lun and Brand, 1998) and *pax8* mutant allele *pax8-RFP* (Ikenaga et al., 2011) are referred to herein as *pax2a*<sup>-/-</sup> and *pax8*<sup>-/-</sup>, respectively. Mutant alleles *sox2*<sup>x50</sup>, *sox3*<sup>x52</sup> and *sox3*<sup>x53</sup> were generated by TALEN and CRISPR/Cas9 technology. TALEN left and right arm constructs were assembled using GoldyTALEN (Bedell et al., 2012), sequences of which are highlighted blue in Fig. 1A. For targeting *sox3*, single strand guide RNA (blue sequence in Fig. 1A) and Cas9 mRNA were co-injected into one-cell stage wild-type embryos that were raised for screening founders. Transgenic lines *TG(hsp70: fgf8a)<sup>x17</sup>*, *TG(hsp70: sox2)<sup>x21</sup>* (Millimaki et al., 2010) and *TG(hsp70: sox3)<sup>x32</sup>* (first described here) were used for gene misexpression and referred to as *hs: fgf8*, *hs: sox2* and *hs: sox3*, respectively. *TG(brn3c: gap43-GFP)* (Xiao et al., 2005) was used to visualize sensory hair cells. Embryos were developed under standard conditions at 28.5 °C (except for heat-shock experiments as noted below) in fish water containing methylene blue and staged based on standard morphological features (Kimmel et al., 1995). Young embryos were co-stained for *myoD* during in situ hybridization to count somites for precise staging. PTU (1-phenyl 2-thiourea, 0.3 mg/ml) was supplemented to fish water to prevent melanin formation in older embryos (> 24 hpf).

### 2.2. Gene misexpression and morpholino injections

Misexpression was accomplished by briefly incubating embryos heterozygous or homozygous for heat-shock inducible transgenes in a water bath at 39 °C for 30 or 60 min (except where noted in the text). Embryos were developed at 33 °C after heat-shock until fixation. Wild-type embryos were also heat shocked to serve as controls in all

misexpression studies. To knock down *sox3*, wild-type embryos were injected at the one-cell stage with varying doses of *sox3*-mo1 (Bricaud and Collazo, 2006), as indicated in the text. In all morpholino knock-down experiments, *p53*-mo (Robu et al., 2007) was co-injected to prevent non-specific cell death. Phenotypes described in this study were examined in at least 15 embryos per probe and time point unless stated otherwise.

### 2.3. In situ hybridization, cell transplantation and data analysis

Whole-mount in situ hybridization was performed as previously described (Phillips et al., 2001). Transgenic donor embryos were injected with lineage tracer (10,000 MW, lysine-fixable tetramethylrhodamine labeled dextran in 0.2 M KCl) at the one-cell stage. Donor cells were then transplanted into non-labeled wild-type host embryos at the late blastula-stage. Quantification of otic vesicle size and gene expression area was performed using Photoshop measuring the number of pixels, and data were normalized relative to wild-type control embryos. The edges of gene expression domains were determined by comparing stained embryos viewed at high magnification with corresponding images in Photoshop. Quantification of anterior expansion distance of ectopic *pax8*-expressing cells was performed using Photoshop by measuring distances in pixels, then converting to microns based on the fold-magnification of the images. Significance was evaluated by students' t-test (pair-wise comparison), or ANOVA and Tukey's post-hoc HSD tests (for experiments involving more than two groups).

### 2.4. RNA extraction, cDNA synthesis and qRT-PCR

For each genotype, RNA was extracted from 24 embryos at 36 hpf using Trizol (Life technologies) and chloroform (MACRON fine chemicals). cDNA were synthesized from 1.5 µg of total RNA using SuperScript First-strand synthesis kit (Invitrogen). To generate a linear range of PCR products, cDNA samples were diluted 1:64 for *sox2* and *sox3* specific amplification, and 1:2048 for *b-actin* (a constitutive control). For each independent experiment, template dilutions were done in triplicate, and each experiment was repeated three times. 10 µl reaction mixtures including PowerUp SYBR green master mix (Applied Biosystems), diluted cDNA and gene specific primers in the ratio of 5:3:2 were dispensed into 96-well plates with optical adhesive covers (Bio-Rad), and run in an Applied Biosystems 7300 real time PCR system using the default protocol. Fold-change for each gene was calculated using the 2<sup>-ΔΔC<sub>T</sub></sup> method. Results from three independent experiments were averaged to calculate means and standard error of means. Data were presented as fold-changes relative to wild-type control mRNA levels. Gene specific primer pairs used for qRT-PCR are as follows: *sox2* 5'-AACGGCTCGCCACCTA-3' and 5'-TCATTC CCGCGTGTCTT-3'; *sox3* 5'-GCCGACCACTCCAGTCTACA-3' and 5'-CTGTCCCTGCGCTTTGATAGT-3'; *b-actin* 5'-AGGTCATCACCAT CGGCAAT-3' and 5'-CAATGAAGGAAGGCTGGAACAG-3'. *sox2*<sup>-/-</sup> homozygous mutant embryos were identified by their characteristic tail phenotype (Fig. 1L) and a deficiency in hair cell accumulation (Gou et al., this issue).

### 2.5. PCR genotyping

To ensure accurate identification of *sox2*<sup>-/-</sup>, *sox3*<sup>-/-</sup> and *pax8*<sup>-/-</sup> mutants, individual embryos were prepared for single-embryo genotyping after phenotype or expression patterns were documented. DNA from single embryos was extracted following methods described previously (Meeker et al., 2007), with addition of a proteinase-K digestion step for embryos older than 12 hpf or fixed embryos processed by in situ hybridization. *sox2* homozygous and heterozygous mutants were identified by PCR using forward primer 5'-CCAGCAAGTTACTTCAACTG-3' and reverse primer 5'-GCAGGGTGTACTTGTCTTCTT-3'. PCR products

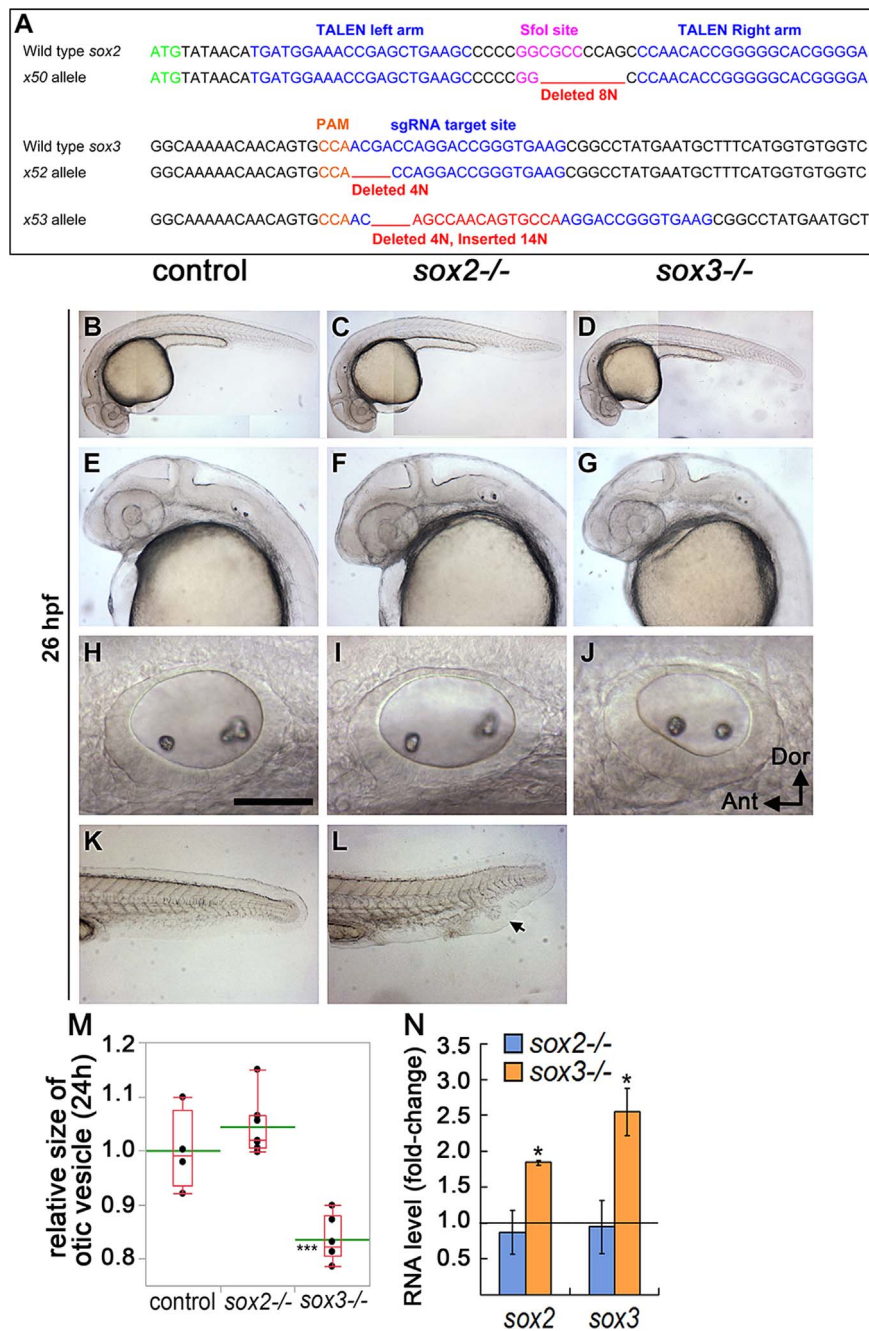


**Fig. 1. Genetic targeting of *sox2* and *sox3*.** (A) Sequences for targeting vectors for *sox2* (TALEN) and *sox3* (sgRNA) and resulting lesions in *sox2* (allele *x50*) and *sox3* (alleles *x52* and *x53*). The deletion in *x50* leads to loss of an SfoI restriction site (magenta), which was used for genotyping, whereas *sox3* indels were identified by allele-specific PCR primers (see Materials & Methods). (B-L) Live embryos at 26 hpf showing general morphology (B-D), cranial development (E-G), tail development (K-L) and the otic vesicle (H-J, lateral views with anterior to the left; Scale bar, 50 μm) in control, *sox2*<sup>-/-</sup> and *sox3*<sup>-/-</sup> mutants. Excess cells at the ventral tip of the tail in *sox2*<sup>-/-</sup> embryos are indicated (arrow). (M) Box-and-whisker plot of surface area of otic vesicle, normalized to control embryos, in control embryos and *sox2*<sup>-/-</sup> and *sox3*<sup>-/-</sup> mutants. Green line indicates mean. Asterisk indicates statistically significant difference relative to control embryos (\*\*\* P < 0.001, Tukey's HSD test). (N) Quantitative real time PCR measurements of fold changes in *sox2* and *sox3* mRNA levels in *sox2*<sup>-/-</sup> and *sox3*<sup>-/-</sup> mutants at 36 hpf normalized to wild-type control embryos. Error bars represent standard error of the means. Asterisks indicate statistically significant differences relative to controls (\* P < 0.05, t-tests).

were then digested with restriction enzyme SfoI or NarI (NEB), yielding wild-type fragments of 330 and 160 bp, while the mutant PCR product remains uncut at 490 bp. To identify *sox3*<sup>x52</sup> mutants, indel-PCR was performed using three primers in a single reaction: forward primer-1 5'-CGTTTCTTTTCGAGTGCTTGGC-3', forward primer-2 (indel primer) 5'-GCAAAAACAACAGTGCCAACGA-3' and reverse primer 5'-TTTGTAAATCCGGGTGCTCCTTC-3'. *sox3*<sup>x52/x52</sup> homozygous mutant DNA yielded a single 344 bp amplicon, while wild-type or *sox3*<sup>x52/+</sup> heterozygous DNA yielded 239 and 344 bp fragments. To identify *pax8*-RFP mutants, forward primer 5'-TCTTCACCCTCACCAGAAATGACC-3'

and reverse primer 5'-ATTGTGTGCATTTATCAGCGCAGTG-3' flanking the DsRed Express insert were used. PCR yielded a ~1.2 kb fragment in *pax8*-RFP homozygous mutants, and a ~300 bp fragment in wild-type embryos.

### 3. Results

#### 3.1. Targeting *sox2* and *sox3*

To evaluate the functions of *sox2* and *sox3* in otic/epibranchial



induction, we used TALEN and CRISPR/Cas9 technology to target *sox2* and *sox3* (Fig. 1A and Materials & Methods). We recovered one lesion for *sox2* (allele *x50*) and two lesions for *sox3* (alleles *x52* and *x53*) that lead to frame shifts near the 5' end of the gene followed by multiple premature stop codons (presumptive null mutations, Fig. 1A). Phenotypes of *sox3<sup>x52/x52</sup>* and *sox3<sup>x53/x53</sup>* are identical, but for simplicity all figures in this paper depict data obtained with *sox3<sup>x52/x52</sup>* mutants, hereafter referred to as *sox3*<sup>-/-</sup> mutants. Both *sox2*<sup>-/-</sup> and *sox3*<sup>-/-</sup> mutants show largely normal morphology at 26 hpf (Fig. 1B–G) except that *sox2*<sup>-/-</sup> mutants show minor growth defects at ventral tip of the tail (Fig. 1L arrow) and *sox3*<sup>-/-</sup> mutants show a 15–20% reduction in the size of the otic vesicle (Fig. 1J, M). During subsequent development *sox2*<sup>-/-</sup> mutants fail to inflate their swim bladders and die around 7–9 dpf, whereas *sox3*<sup>-/-</sup> mutants subsequently recover and grow into healthy fertile adults with no obvious morphological or behavioral abnormalities.

Because such mutations sometimes lead to nonsense-mediated decay of mutant transcript, we performed quantitation of *sox2* and *sox3* transcript levels in mutant embryos. *sox2*<sup>-/-</sup> mutants show no significant changes in accumulation of *sox2* or *sox3* transcript levels (Fig. 1N). Surprisingly, *sox3*<sup>-/-</sup> mutants show a nearly two-fold increase in *sox2* transcript levels and a 2.5-fold increase in *sox3* transcript levels (Fig. 1N). Elevation of *sox2* mRNA levels in *sox3*<sup>-/-</sup> mutant could ameliorate the phenotype, possibly contributing to their ability to recover and survive.

### 3.2. Early placodal expression of *sox2*

We previously reported that otic expression of *sox2* begins around 14 hpf (10 somite-stage), just after the otic placode becomes morphologically visible (Millimaki et al., 2010). However, subsequent analysis revealed that weak otic/epibranchial expression of *sox2* can be detected in up to a third of wild-type embryos by 12–12.5 hpf (6–7 somites stage) (Fig. 2A). In *sox3*<sup>-/-</sup> mutants the onset of otic/epibranchial expression of *sox2* was normal, but expression was more intense and fully penetrant (Fig. 2B), consistent with higher *sox2* transcript abundance in this background. Similarly, the intensity of early expression of *sox2* increased in all embryos following misexpression of *fgf8* at 10 hpf (Fig. 2C). These findings are consistent with the possibility that *sox2* cooperates with *sox3* in regulating early otic/epibranchial development.

### 3.3. Effect of loss of *sox2* and *sox3* in early otic and epibranchial placode

In close agreement with the effects of morpholino knockdown of *sox3* (Padanad and Riley, 2011), *sox3*<sup>-/-</sup> mutants show a 20% decrease in the otic domain of *pax8* at 11 hpf and a similar decrease in the otic domain of *pax2a* at 12 hpf (Fig. 3C, G, I, J). The deficiency in otic tissue persists through at least 26 hpf (Fig. 1J), confirming that *sox3* is required for normal otic induction. In *sox2*<sup>-/-</sup> mutants, otic expression

of *pax8* is normal whereas the domain of *pax2a* at 12 hpf is reduced by about 15% (Fig. 3B, F, I, J), consistent with the later onset of *sox2* expression. This shows that *sox2* is also required for normal otic induction, although *sox2*<sup>-/-</sup> mutants recover to form a morphologically normal otic vesicle by 26 hpf (Fig. 1I). In *sox2*<sup>-/-</sup>; *sox3*<sup>-/-</sup> double mutants, the otic domain of *pax8* is reduced by 33% (Fig. 3D, I), although this deficiency is not significantly worse than in *sox3*<sup>-/-</sup> mutants (*p*=0.06). Likewise, the otic domain of *pax2a* is reduced by 22% in *sox2*<sup>-/-</sup>; *sox3*<sup>-/-</sup> double mutants, which is similar to the deficiency in *sox3*<sup>-/-</sup> mutants (Fig. 3H, J). Thus, the weak early expression of *sox2* has little effect on early otic development in the absence of *sox3*. Additionally, the two-fold increase in *sox2* transcript accumulation seen in *sox3*<sup>-/-</sup> mutants apparently does not ameliorate the early deficiency in otic development.

We next examined development of epibranchial ganglia at 36 hpf, marked by expression of *phox2a* (Begbie et al., 1999; Lee et al., 2003; Nechiporuk et al., 2005). In keeping with previous *sox3* knockdown experiments (Padanad and Riley, 2011), *sox3*<sup>-/-</sup> mutants show deficiencies in all epibranchial ganglia at 36 hpf, especially in the facial ganglion which was reduced by 80% (Fig. 4C, E). *sox2*<sup>-/-</sup> mutants showed slight but non-significant deficiencies in epibranchial ganglia (Fig. 4B, E). However, *sox2*<sup>-/-</sup>; *sox3*<sup>-/-</sup> double mutants show much more pronounced deficiencies compared to *sox3*<sup>-/-</sup> mutants (Fig. 4D, E). For example, some *sox2*<sup>-/-</sup>; *sox3*<sup>-/-</sup> double mutants showed complete ablation of the facial (3/6 specimens) and glossopharyngeal ganglia (1/6 specimens). We also examined expression of *pax2a* at 24 hpf, which marks epibranchial placodes prior to the onset of neurogenesis. While wild-type embryos show four discrete patches of *pax2a* expression, *sox2*<sup>-/-</sup>; *sox3*<sup>-/-</sup> double mutants show marked deficiencies in anterior patches of *pax2a* corresponding to facial and glossopharyngeal placodes (Fig. 4F, G). Together, these data show that *sox2* and *sox3* cooperate and are required to establish a full complement of both otic and epibranchial placodal tissue.

### 3.4. Interactions with *pax8*

The above data show that *sox3*<sup>-/-</sup> mutants largely recapitulate our previously reported *sox3*-morphant phenotype, but we also wished to compare the phenotypes of *pax8*-morphants and *pax8*<sup>-/-</sup> mutants (Padanad and Riley, 2011). In *pax8*<sup>-/-</sup> mutants, the otic domain of *pax2a* at 12 hpf is reduced by 30% (Fig. 5B, D), consistent with previous morpholino data. In *pax8*<sup>-/-</sup>; *sox3*<sup>-/-</sup> double mutants the *pax2a* domain is reduced by 32%, which is not statistically different from *pax8*<sup>-/-</sup> mutants (Fig. 5C, D). This is in contrast to *pax8*-*sox3* double morphants, which show an additive reduction in the *pax2a* domain relative to *pax8*-morphants (Padanad and Riley, 2011). We also examined the interaction between *pax8* and *pax2a*. We found that *pax8*<sup>-/-</sup>; *pax2a*<sup>-/-</sup> double mutants undergo placode induction but later show severe deficiency of otic tissue, producing very small otic vesicles by 24 hpf (Fig. 6C, F, I, L). In contrast, injection of *pax8*-mo into *pax2a*<sup>-/-</sup> mutants usually eliminates formation of a morphological

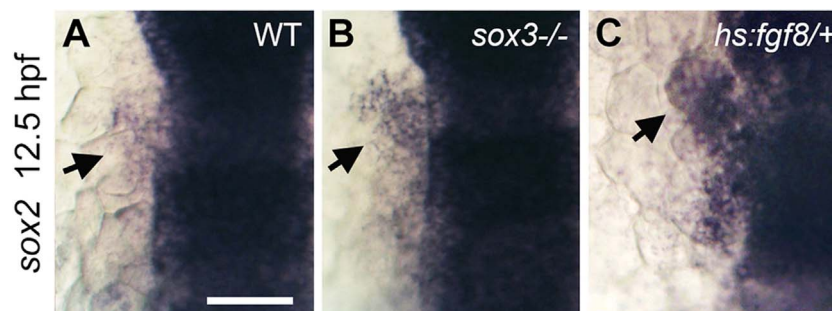


**Fig. 2. Early placodal expression of *sox2*.** Otic/epibranchial *sox2* expression (arrows) at 12.5 hpf in a wild-type embryo (A), a *sox3*<sup>-/-</sup> mutant (B) and a *hs:fgf8*/+ transgenic embryo (C) heat shocked at 10 hpf, 39 °C for 30 min. Dorsal views with anterior up, lateral to the left. Scale bar, 100 μm.

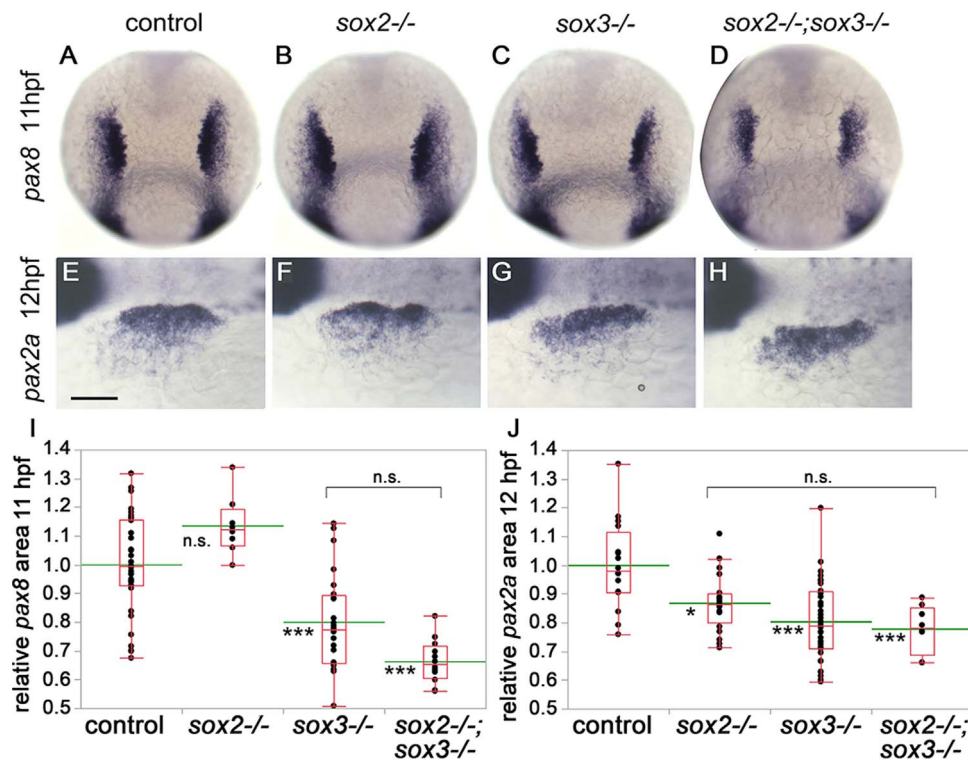


**Fig. 3.** Effect of *sox2*<sup>-/-</sup> and *sox3*<sup>-/-</sup> on early placode size. (A-H) Expression of *pax8* at 11 hpf (A-D) and *pax2a* at 12 hpf (E-H) in control embryos (A, E), *sox2*<sup>-/-</sup> mutants (B, F), *sox3*<sup>-/-</sup> mutants (C, G) and *sox2*<sup>-/-</sup>; *sox3*<sup>-/-</sup> double mutants (D, H). Dorsal views with anterior up (A-D) or dorsal-lateral views with anterior to the left (E-H). Scale bar (E-H), 100  $\mu$ m. (I, J) Box-and-whisker plots of relative surface area of otic/epibranchial domain of *pax8* (I) or *pax2a* (J) in control, *sox2*<sup>-/-</sup>, *sox3*<sup>-/-</sup> and *sox2*<sup>-/-</sup>; *sox3*<sup>-/-</sup> double mutant embryos. Data are normalized relative to control groups, with means indicated by green lines. Asterisks indicate statistically significant differences relative to control (\*P < 0.05, \*\*\* P < 0.001, Tukey's HSD test). Brackets indicate comparisons between non-control groups. n.s., not significantly different.

vesicle, although a small number of scattered otic cells persist (Hans et al., 2004). We draw several conclusions from these data. First, the *sox3*<sup>-/-</sup> and *pax8*<sup>-/-</sup> mutant phenotypes generally validate phenotypes produced by corresponding morpholinos when used singly, although combining these morpholinos produces an excessively severe phenotype probably reflecting additive off-target effects. Second, mutant analysis confirms that *pax8* is required to establish a normally sized

placode; and *pax8* and *pax2a* are together required to maintain otic fate by the majority of otic cells. Third, mutant analysis suggests that *sox3* and *pax8* operate in the same genetic pathway, but *pax8* function is more critical.

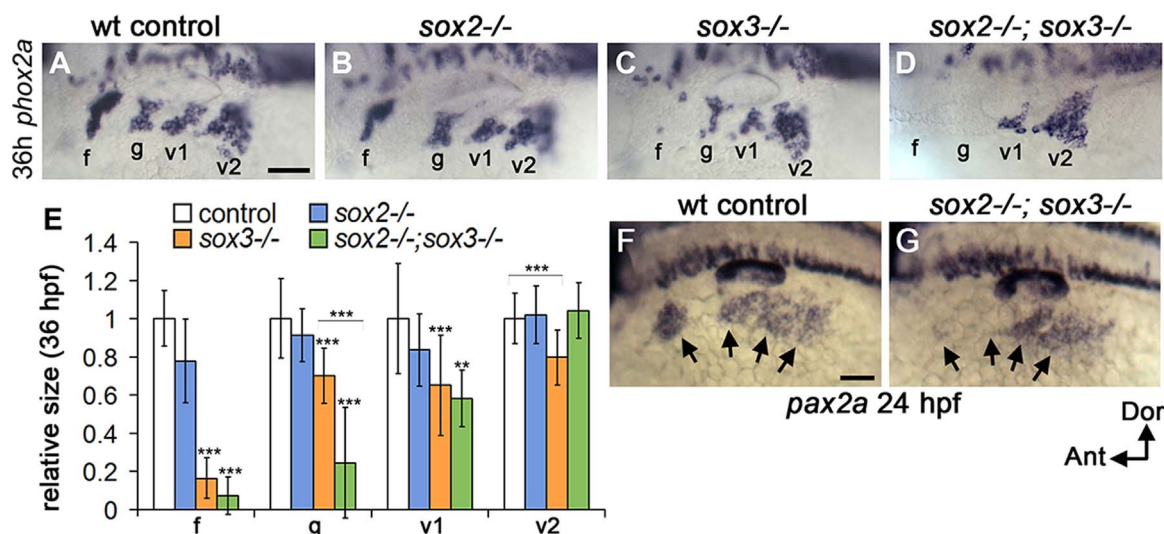


**Fig. 4.** Effect of *sox2*<sup>-/-</sup> and *sox3*<sup>-/-</sup> on epibranchial ganglia. (A-D) Expression of *phox2a* at 36 hpf in a wild-type embryo (A), *sox2*<sup>-/-</sup> (B), *sox3*<sup>-/-</sup> (C) and *sox2*<sup>-/-</sup>; *sox3*<sup>-/-</sup> double mutant (D) embryo. Locations of the facial (f), glossopharyngeal (g), and vagal (v1 and v2) ganglia are indicated. Dorsal-lateral views with anterior to the left. (E) Quantitation of relative surface area of *phox2a* expression in individual epibranchial ganglia in control, *sox2*<sup>-/-</sup>, *sox3*<sup>-/-</sup> and *sox2*<sup>-/-</sup>; *sox3*<sup>-/-</sup> double mutant embryos. Data show means and standard deviations normalized to wild-type controls. Asterisks indicate statistically significant differences relative to controls (\*\*P < 0.01, \*\*\*P < 0.001, Tukey's HSD test), or between non-control groups (bracket). (F, G) Dorsolateral views (anterior to left) showing expression of *pax2a* at 24 hpf in a control embryo (F) and *sox2*<sup>-/-</sup>; *sox3*<sup>-/-</sup> double mutant (G). Arrows indicate positions of epibranchial placodes. Scale bars, 50  $\mu$ m.

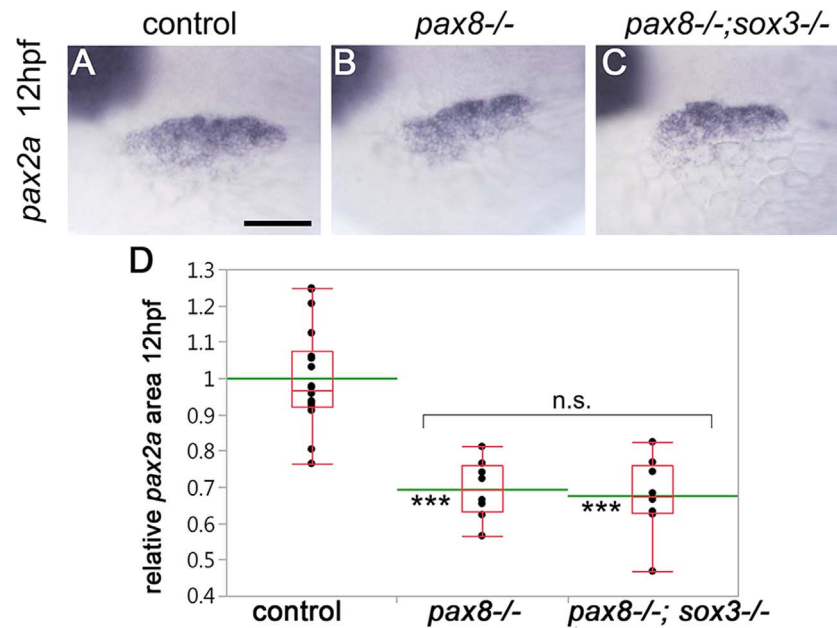


**Fig. 5. Interaction between *pax8*<sup>-/-</sup> and *sox3*<sup>-/-</sup> during early placode development.** (A–C) Expression of *pax2a* at 12 hpf in a wild-type control embryo (A), a *pax8*<sup>-/-</sup> mutant (B) and a *pax8*<sup>-/-</sup>; *sox3*<sup>-/-</sup> double mutant (C) embryo. Dorsal-lateral view with anterior to the left. Scale bar, 50  $\mu$ m. (D) Box-and-whisker plot of relative surface area of otic/epibranchial domain of *pax2a* at 12 hpf in control, *pax8*<sup>-/-</sup> and *pax8*<sup>-/-</sup>; *sox3*<sup>-/-</sup> double mutant embryos. Data are normalized relative to control groups, with means indicated by green lines. Asterisks indicate statistically significant differences relative to controls (\*\*\*  $P < 0.001$ , Tukey's HSD test). n.s., not significantly different.

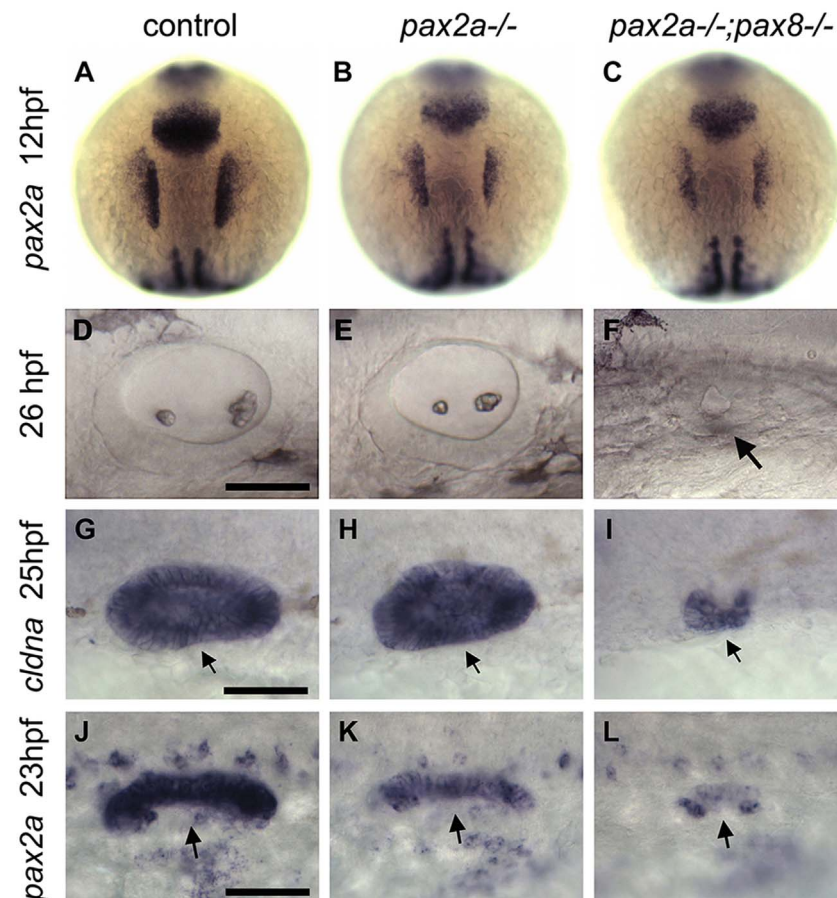


**Fig. 6. Interaction between *pax8*<sup>-/-</sup> and *pax2a*<sup>-/-</sup> during otic development.** (A–C) Expression of *pax2a* at 12 hpf in control (A), *pax2a*<sup>-/-</sup> (B) and *pax2a*<sup>-/-</sup>; *pax8*<sup>-/-</sup> (C) embryos (dorsal views, anterior to the top). Staging of embryos was confirmed by *myoD* expression in somites. (D–F) Lateral views (anterior to left) of the otic vesicle in control (D), *pax2a*<sup>-/-</sup> (E) and *pax2a*<sup>-/-</sup>; *pax8*<sup>-/-</sup> (F) embryos imaged live at 26 hpf. The small otic vesicle in the *pax2a*<sup>-/-</sup>; *pax8*<sup>-/-</sup> double mutant (F) is marked with an arrow. (G–L) Dorsal views (anterior to left) showing expression of *cldna* (G–I) and *pax2a* (J–L) at 25 hpf and 23 hpf respectively in control (G, J), *pax2a*<sup>-/-</sup> (H, K) and *pax2a*<sup>-/-</sup>; *pax8*<sup>-/-</sup> (I, L) embryos. Arrows indicate otic expression domains. Scale bars (D–L), 50  $\mu$ m.



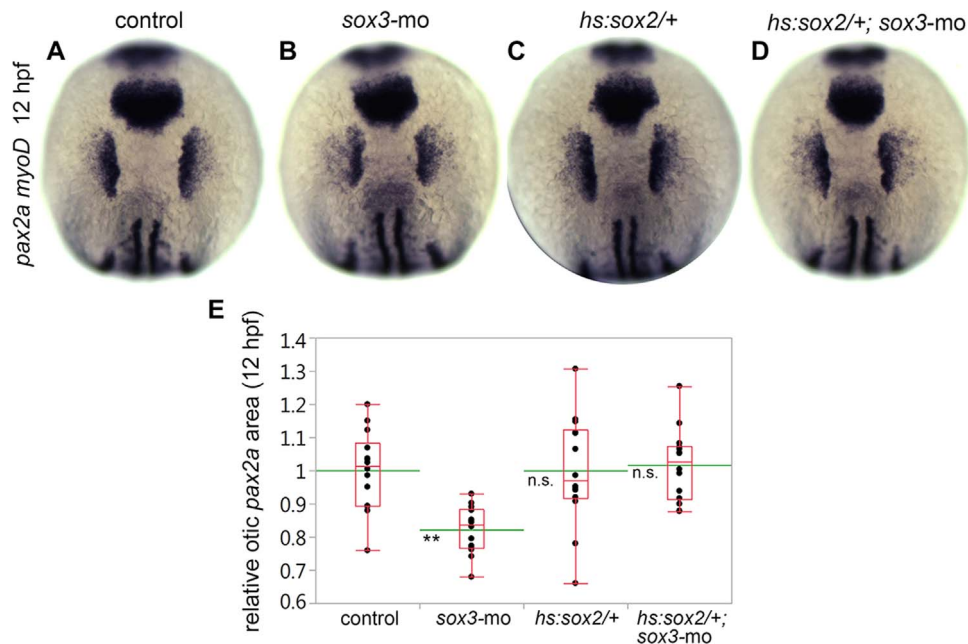


**Fig. 7. *sox2* can substitute for *sox3* during early otic development.** (A–D) Dorsal views (anterior to the top) showing expression of *pax2a* at 12 hpf in a control embryo (A), a *sox3*-morphant (B), a *hs:sox2/+* heterozygote (C) and *hs:sox2/+* heterozygote injected with *sox3*-mo (D). Embryonic staging was confirmed with *myoD* expression in somites. Embryos were heat shocked at 35 °C from 10 to 12 hpf. *sox3*-morphants in (B) and (D) were injected with 5 ng each of *sox3*-mo. (E) Box-and-whisker plots of relative surface area of the otic/epibranchial domain of *pax2a* at 12 hpf in controls, *sox3*-morphants, *hs:sox2/+* heterozygotes and *hs:sox2/+* heterozygotes injected with *sox3*-mo. Data are normalized relative to control groups, with means indicated by green lines. Asterisks indicate statistically significant differences compare to control (\*\*  $P < 0.01$ , Tukey's HSD test). n.s., no significant difference compared to controls.

### 3.5. Redundancy between *sox2* and *sox3*

To further address *sox2* and *sox3* function, we generated heat shock-inducible transgenes for both genes. Although *sox2*<sup>-/-</sup>; *sox3*<sup>-/-</sup> double mutants are similar to *sox3*<sup>-/-</sup> mutants, we reasoned that the inability of *sox2* to compensate for loss of *sox3* reflects the relatively low level of *sox2* expression during early placodal development. To test this possibility, we injected *sox3*-mo into *hs:sox2/+* embryos to determine whether transgenic *sox2* can rescue early placodal deficiencies caused by loss of *sox3*. For this experiment we used a low level of heat shock (35 °C from 10 to 12 hpf) to avoid defects caused by high-level misexpression of *sox2* (see below). qRT-PCR analysis showed that this regimen caused a 5–6 fold increase in *sox2* transcript abundance when measured 40 min or 60 min after initiating heat shock (relative to non-transgenic *sox3*-morphants). Non-transgenic *sox3*-morphants showed an 18% reduction in the otic domain of *pax2a* at 12 hpf, similar to *sox3*<sup>-/-</sup> mutants (Fig. 7B, E). Weak activation of *hs:sox2* by itself had no effect on otic development but was sufficient to restore the otic domain of *pax2a* to normal in *sox3*-morphants (Fig. 7C, D, E). This supports the idea that *sox2* can substitute for *sox3* during early otic development.

### 3.6. Misexpression of *sox2* and *sox3*

To further explore the functions of *sox2* and *sox3* during otic placode development, we tested the effects of misexpressing *sox2* or *sox3* at different developmental stages and expression levels using heat shock-inducible transgenes. For moderate misexpression we heat shocked *hs:sox2/+* or *hs:sox3/+* transgenic heterozygotes at 39 °C for 60 min, and for high-level misexpression we heat shocked embryos homozygous for the transgene. These regimens lead to a pulse of overexpression that peaks just after the end of the heat shock interval and decays gradually over the next several hours (Padanad et al., 2012). Moderate misexpression of *sox2* or *sox3* at 9 hpf led to strong reduction or elimination of otic expression of *pax8* and *pax2a* at 12 hpf, indicating strong repression of otic differentiation (Fig. 8A–F).

Moderate misexpression of *sox2* at 12 hpf, after otic differentiation has already begun, did not alter otic expression of *pax2a* or *pax8* at 14 hpf (Fig. 8H, K). However, high-level misexpression of *sox2* at 12 hpf attenuated otic expression of *pax8* and reduced the size of the otic domain of *pax2a* at 14 hpf (Fig. 8I, L). In general the effects of misexpressing *sox3* were more pronounced than *sox2*. For example, moderate misexpression of *sox3* at 12 hpf eliminated expression of *pax8* by 14 hpf and expression of *pax2a* was nearly abolished as well (data not shown). Because global misexpression of *sox2* or *sox3* could disrupt essential signaling interactions with surrounding tissues, we generated mosaic embryos by transplanting lineage-labeled transgenic cells into unlabeled wild-type host embryos. When mosaic embryos were heat shocked at 9 hpf, transplanted *hs:sox2/+* or *hs:sox3/+* cells showed little or no otic expression of *pax8* or *pax2a* by 11 hpf, whereas surrounding wild-type cells expressed otic markers normally (Fig. 9A–B', E–H'). In contrast, when mosaic embryos were heat shocked at 12 hpf, transplanted *hs:sox2/hs:sox2* cells and *hs:sox3/+* cells showed normal otic expression of *pax2a* at 14 hpf (Fig. 9C, D, I, J). These data suggest that increasing expression of *sox2* or *sox3* at 9 hpf cell-autonomously blocks otic induction, whereas elevating *sox2* or *sox3* at 12 hpf has little effect, indicating that otic fate is stably specified.

### 3.7. Otic induction requires an optimal level of *sox3* expression

During normal otic induction, *sox3* is induced at a high level in the initial response to Fgf, and subsequently *sox3* expression declines to a discrete lower level in response to rising Fgf levels (Padanad and Riley, 2011). We previously reported that moderate misexpression of *fgf3* or *fgf8* at 10 hpf leads to strong ectopic expression of *sox3* throughout anterior preplacodal ectoderm, but ectopic *pax8* is not co-induced under these conditions (Padanad et al., 2012). In contrast, high-level misexpression of *fgf3* or *fgf8* leads to a reduced domain of ectopic *sox3*, as well as ectopic expression of *pax8*, *pax2a*, and other otic markers in anterior preplacodal ectoderm. We hypothesized that the high level of ectopic *sox3* induced by moderate Fgf repressed co-induction of *pax8*, whereas the lower level of *sox3* induced by high-level Fgf facilitated

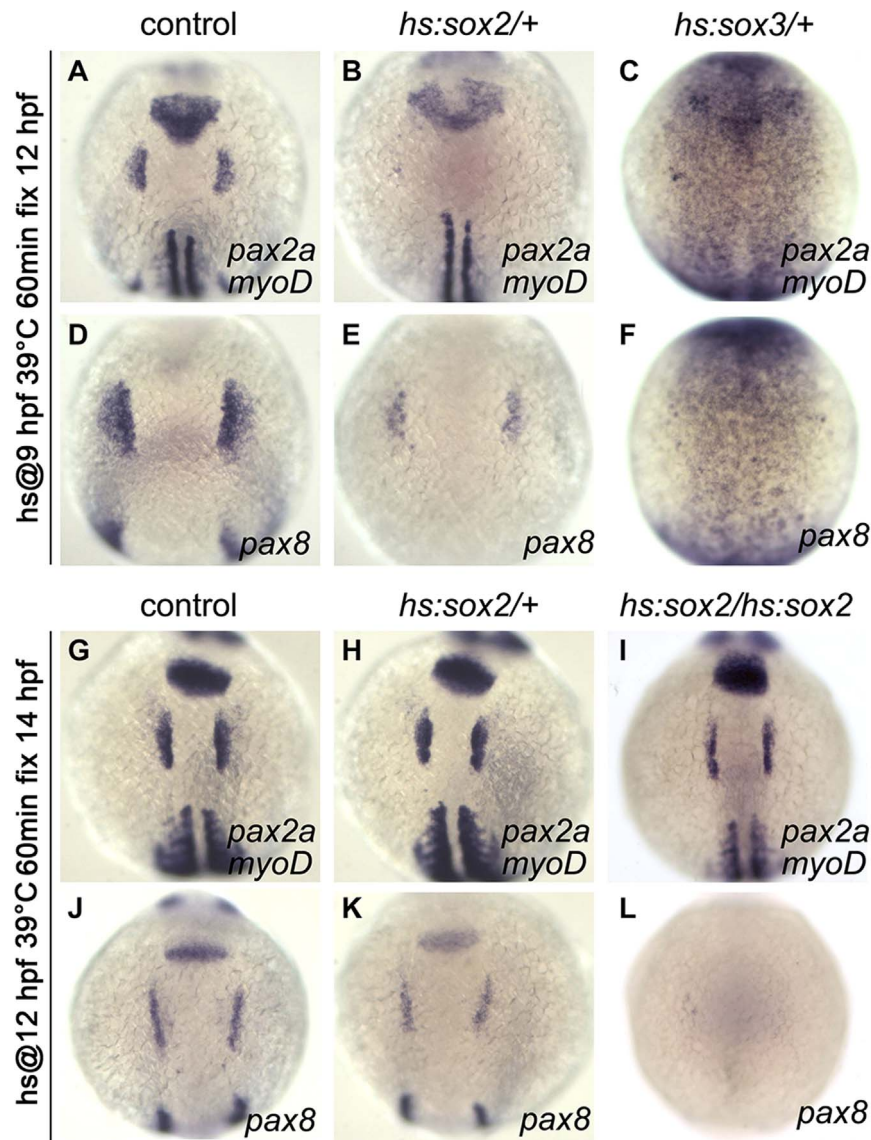


**Fig. 8. Global misexpression of *sox2* or *sox3*.** (A–F) Expression of *pax2a* (A–C) and *pax8* (D–F) at 12 hpf in control embryos (A, D), *hs:sox2/+* heterozygotes (B, E) and *hs:sox3/+* heterozygotes (C, F) that were heat shocked at 9 hpf, 39 °C for 60 min. (G–L) Expression of *pax2a* (G–I) and *pax8* (J–L) at 14 hpf in control embryos (G, J), *hs:sox2/+* heterozygotes (H, K) and *hs:sox2/hs:sox2* homozygotes (I, L) that were heat shocked at 12 hpf, 39 °C for 60 min. Embryonic staging was confirmed with *myoD* expression in somites. All images show dorsal views with anterior to the top.

ectopic induction of multiple otic markers. To test this, we injected *sox3*-mo at varying concentrations into *hs: fgf8/+* embryos to titrate the level of ectopic *sox3* activity following moderate misexpression of Fgf8. When *hs: fgf8/+* embryos were injected with a low dose (0.75 ng) of *sox3*-mo and then heat shocked at 10 hpf (39 °C for 30 min), ectopic *pax8*-expressing cells were detected an average of 220  $\mu$ m anterior to the midbrain-hindbrain border, nearly to the front of the head, compared to only 148  $\mu$ m for uninjected *hs: fgf8* embryos (Fig. 10B, C, E). Similarly, the number of ectopic *pax8*-expressing cells produced in *hs: fgf8/+* embryos injected with 0.75 ng *sox3*-mo was on average 40% greater than in uninjected *hs: fgf8/+* embryos. Thus, partial knockdown of *sox3* enhanced the ability of *hs: fgf8* to induce ectopic otic tissue. On the other hand, injecting 2.5 ng *sox3*-mo into *hs: fgf8/+* embryos (to mimic *sox3*<sup>-/-</sup>) reduced the anterior limit of ectopic *pax8* expression to 129  $\mu$ m beyond the midbrain-hindbrain border, corresponding to 33% fewer ectopic *pax8*-expressing cells compared to uninjected *hs: fgf8/+* embryos. The level of ectopic *pax8* expression also appeared much lower in embryos injected with 2.5 ng *sox3*-mo. These data support the hypothesis that a high level of ectopic *sox3* following moderate misexpression of Fgf hinders the ability to induce

ectopic otic tissue. Furthermore, complete knockdown of *sox3* is even more detrimental to ectopic otic induction, whereas weak knockdown of *sox3* potentiates ectopic otic induction. These data are consistent with the idea that proper otic induction requires *sox3*, but the level of *sox3* must be tightly modulated to avoid suppression of differentiation.

#### 4. Discussion

We generated targeted knockouts and heat shock-inducible transgenic lines to evaluate the roles of *sox2* and *sox3* in development of otic and epibranchial placodes in zebrafish. Placodal expression of *sox2* had not been previously reported but we show here that its expression can be detected by early somitogenesis stages, several hours after the onset of *sox3* expression. Mutant analysis confirms that both *sox2* and *sox3* are required for normal development of otic and epibranchial placodes. Moreover, these factors show some degree of redundancy. Mild misexpression of *sox2* rescues the otic placode deficiency in *sox3*<sup>-/-</sup> mutants, and *sox2*<sup>-/-</sup>; *sox3*<sup>-/-</sup> double mutants show a significantly greater deficiency of epibranchial ganglia than single mutants. Although both factors are required, several observations show that



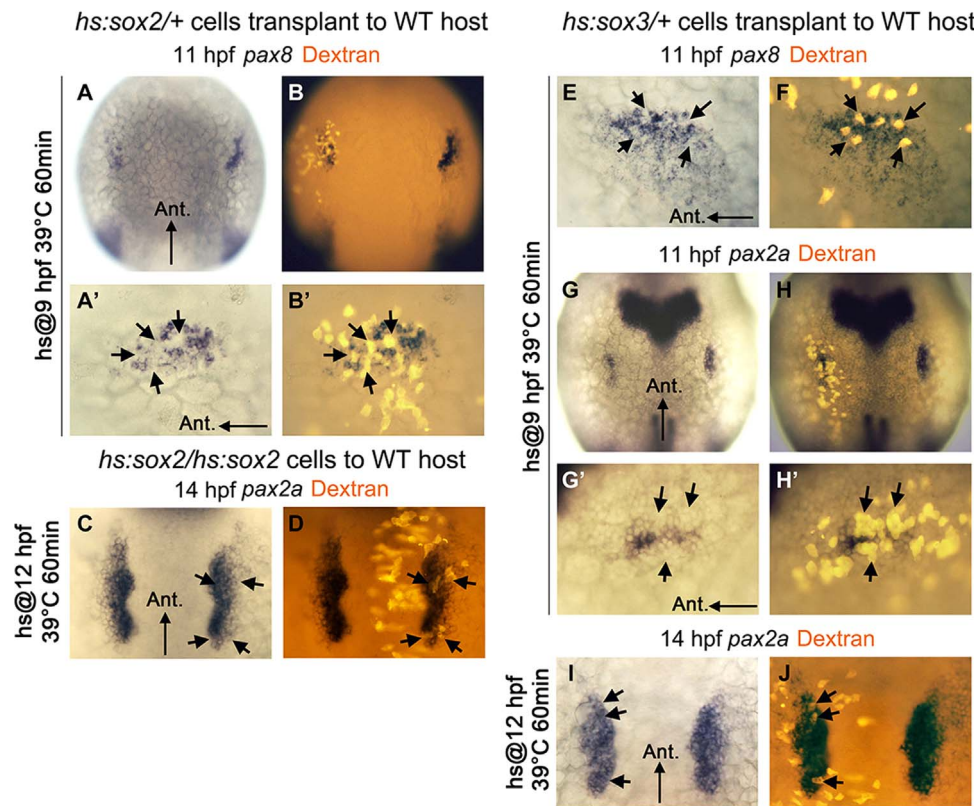


**Fig. 9. Mosaic misexpression of *sox2* or *sox3*.** (A–B') Expression of *pax8* at 11 hpf in a wild-type host embryo into which fluorescent dextran-labeled *hs:sox2/+* transgenic cells were transplanted. The embryo was heat shocked at 9 hpf, 39 °C for 60 min. Bright-field (A, A') and fluorescent (B, B') images of the same specimen. An enlargement of the left otic placode (A', B') shows the positions of transgenic cells (arrows). (C, D) Bright-field (C) and fluorescent (D) images showing *pax2a* expression at 14 hpf in a wild-type host embryo with fluorescent dextran-labeled *hs:sox2/hs:sox2* transgenic cells (indicated by arrows). The embryo was heat shocked at 12 hpf, 39 °C for 60 min. (E, F) Bright-field (E) and fluorescent (F) images showing *pax8* expression in the otic placode at 11 hpf in a wild-type host embryo with fluorescent dextran-labeled *hs:sox3/+* transgenic cells. The embryo was heat shocked at 9 hpf, 39 °C for 60 min, and the positions of transgenic cells are indicated (arrows). (G–H') Bright-field (G, G') and fluorescent (H, H') images showing *pax2a* expression at 11 hpf in a wild-type host embryo with fluorescent dextran-labeled *hs:sox3/+* transgenic cells. The embryo was heat shocked at 9 hpf, 39 °C for 60 min. An enlargement of the left otic placode (G', H') shows positions of transgenic cells (arrows). (I, J) Bright-field (I) and fluorescent (J) images showing *pax2a* expression at 14 hpf in a wild-type host embryo with fluorescent dextran-labeled *hs:sox3/+* transgenic cells. The embryo was heat shocked at 12 hpf, 39 °C for 60 min. Positions of transgenic cells are indicated (arrows).

the overall level of *sox2* and *sox3* expression must not exceed an upper limit during early placodal development. High-level misexpression of *sox2* or *sox3* cell-autonomously blocks initial otic induction but does not block or reverse otic fate after otic cells have begun to differentiate. Moreover, in an assay to induce ectopic otic tissue, partial knockdown of *sox3* enhances the ability of Fgf misexpression to induce ectopic *pax8* whereas full knockdown of *sox3* strongly inhibits this response. Together these data show that an optimal level of *sox2* and *sox3* are required for proper induction of otic and epibranchial placodes, with either higher or lower levels becoming inhibitory.

We also reexamined the genetic interaction between *sox3* and *pax8*. The otic placode deficiency seen in *pax8*<sup>-/-</sup> mutants is similar to *pax8*<sup>-/-</sup>; *sox3*<sup>-/-</sup> double mutants, suggesting that *pax8* and *sox3* act in the same genetic pathway. This is in contrast to *pax8*-*sox3* double morphants, which show an additive deficiency of otic tissue. Thus, while *sox3*<sup>-/-</sup> and *pax8*<sup>-/-</sup> morphant phenotypes closely resemble corresponding mutant phenotypes, the double morphant phenotype appears too severe and probably reflects additive off-target effects.

#### 4.1. A common *Pax2/8*-*Sox2/3* pathway

How do Pax8 and Sox3 work together to promote otic induction? One possibility is that Pax8 and Sox3 bind independently to a common set of enhancers of early otic genes, with both factors being required for full activation. Alternatively, Sox3 and Pax8 could form heterodimers required for enhancer binding. An analogous situation has been documented during development of the lens placode, in which Sox2 and Pax6 dimerize to bind the DC5 lens enhancer (Kamachi et al.,

2001). Binding is cooperative such that loss of either factor severely attenuates transcription. This accounts for why loss of either *Sox2* or *Pax6* blocks lens placode development at a very early stage (Smith et al., 2009). A similar *Sox2*-*Pax6* partnership maintains neural progenitors in the olfactory epithelium (Guo et al., 2010; Packard et al., 2016), although only *Pax6* is required to establish the olfactory placode (Hogan et al., 1988). By comparison, induction of otic/epibranchial placodes is less critically dependent on *sox3* and *pax8*, partly reflecting greater genetic redundancy in otic/epibranchial placodes. Disruption of both *pax8* and *pax2a* leads to gradual loss of most otic cells by 24 hpf (Fig. 5, and Hans et al., 2004), and simultaneous knockdown of a third homolog *pax2b* leads to loss of all otic cells through dedifferentiation (Mackereth et al., 2005). Disruption of *sox2* and *sox3* has much milder effects on placode development, perhaps similar to the role of *Sox2* in the olfactory epithelium but marking a distinct difference from the lens placode.

#### 4.2. Redundancy and compensation between *sox2* and *sox3*

Although zebrafish *sox3*<sup>-/-</sup> mutants are viable and fertile, it is noteworthy that these mutants show roughly 2-fold upregulation of *sox2* (Fig. 1), which could compensate for loss of *sox3*. Such compensation does not ameliorate the early otic deficiency in *sox3*<sup>-/-</sup> mutants since simultaneous loss of *sox2* does not worsen the phenotype. Nevertheless, compensation from *sox2* could facilitate restoration of normal otic development during later stages of development in *sox3*<sup>-/-</sup> mutants. Interestingly, *Sox3* knockout mice are also viable, but in this case there is no detectable upregulation of *Sox2* (Adikusuma et al.,

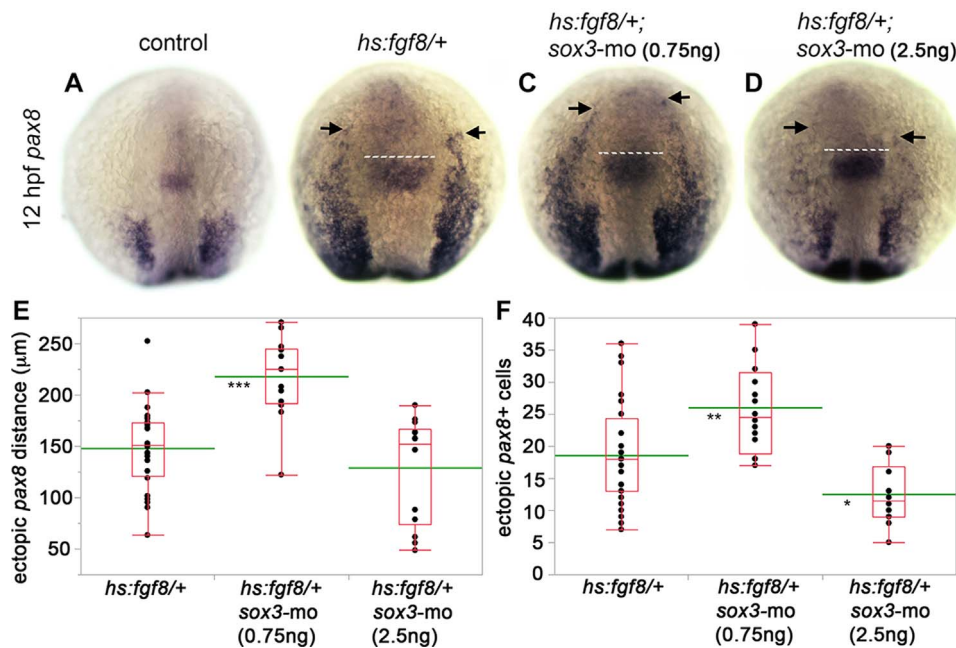


**Fig. 10. Ectopic otic induction requires an optimal level of *sox3*.** (A–D) Expression of *pax8* at 12 hpf in a control (A), *hs:fgf8/+* heterozygote (B), *hs:fgf8/+* heterozygote injected with 0.75 ng *sox3-mo* (C) and *hs:fgf8/+* heterozygote injected with 2.5 ng *sox3-mo* (D) embryo. Embryos were heat shocked at 10 hpf, 39 °C for 30 min. The anterior edge of the midbrain-hindbrain boundary (dashed white line) was used as a reference to measure ectopic expression of *pax8*. Arrows mark the anterior limit of ectopic *pax8* expression (B–D). (E) Box-and-whisker plot of the distance from midbrain-hindbrain border to the anterior limit of ectopic *pax8* expression in *hs:fgf8/+* heterozygotes, *hs:fgf8/+* heterozygotes injected with 0.75 ng *sox3-mo* and *hs:fgf8/+* heterozygotes injected with 2.5 ng *sox3-mo*. (F) Box-and-whisker plot of the number (per side) of ectopic *pax8*-expressing cells anterior to the midbrain-hindbrain border in *hs:fgf8/+* heterozygotes, *hs:fgf8/+* heterozygotes injected with 0.75 ng *sox3-mo* and *hs:fgf8/+* heterozygotes injected with 2.5 ng *sox3-mo*. The green line indicates the mean. Asterisks indicate statistically significant differences compare to control (\*  $P < 0.05$ , \*\*  $P < 0.01$ , \*\*\*  $P < 0.001$ , Tukey's HSD test).

2017). Otic development is expected to be normal in *Sox3* mutants since *Sox3* is not detectably expressed in otic cells in mouse. Of the three *SoxB1* genes in mouse, only *Sox2* is expressed during early otic cells by the otic placode/otic cup stage. Unfortunately, conditional knockouts of mouse *Sox2* have not been conducted early enough to evaluate potential deficiencies in otic placode formation. On the other hand, knockouts induced during early otic vesicle stage block development of neurons and sensory epithelia (Kiernan et al., 2005; Steevens et al., 2017). At later stages in zebrafish, *sox2* and *sox3* act non-redundantly to regulate development of sensory epithelia and neurons, respectively (Gou et al., this issue).

#### 4.3. Sensitivity to *Sox2/Sox3* concentration

There are two general mechanisms by which *Sox2/Sox3* concentration critically affects functional output. First, *Sox2* has been shown to act as a “pioneer factor” that can open large tracts of condensed chromatin (Soufi et al., 2015). *Sox2* has the unusual ability to recognize specific and non-specific sequences on DNA wrapped around nucleosomes, as well as distinct consensus sites within open DNA. Binding to these sites is differentially sensitive to concentration. Therefore, elevating *Sox2* levels could open larger sized tracts of chromatin and bind a wider array of sequences, potentially activating expression of repressors that antagonize normal otic development.

Second, *SoxB1* function is often modified by interacting with other cofactors, with functional output being highly sensitive to modest changes in concentration (Kondoh and Kamachi, 2010; Rizzino and Wuebben, 2016). In embryonic stem cells, for example, the concentration of *Sox2* and *Oct4* must be maintained within a narrow range to maintain pluripotency (Rizzino and Wuebben, 2016). *Sox2* and *Oct4* bind cooperatively into multi-subunit complexes that activate transcription of their own genes, as well as other pluripotency genes (Ambrosetti et al., 1997; Boer et al., 2007; Chew et al., 2005). In this way, *Sox2* and *Oct4* establish a self-reinforcing gene regulatory network that maintains pluripotency. However, when *Sox2* levels are

further elevated, its occupancy on relevant enhancers increases and leads to repression of all genes in the network (Boer et al., 2007; Kopp et al., 2008). This constitutes a binary switch that, once tripped, inhibits pluripotency and initiates differentiation. The mechanism of *Sox2*'s repressor activity is unknown but requires its C-terminal transactivation domain (Boer et al., 2007). Though historically associated with activation, this domain can also bind transcriptional repressors such as HDAC1 and HDAC2 (Cox et al., 2010).

*Sox2* levels are also critical for tissue-progenitors during later stages of development, but the dose-response is opposite to that seen in embryonic stem cells. Specifically, high levels of *Sox2* are required to maintain pluripotency of tissue-specific progenitors whereas lower levels promote differentiation (Gómez-López et al., 2011; Hutton and Pevny, 2011; Juuri et al., 2012; Matsushima et al., 2011; Packard et al., 2016; Tucker et al., 2010). The switch to differentiation involves changes in *Sox2*-partner binding (Kondoh and Kamachi, 2010), but how this relates to *Sox2* concentration remains unknown.

There has been much less molecular analysis of *Sox3* but it is believed to function in tissue-progenitors in a manner similar to *Sox2* (Stavridis et al., 2007; Wang et al., 2006). Indeed, conditional knockout of *Sox2* in mouse leads to compensatory upregulation of *Sox3*, which is thought to ameliorate the phenotype (Miyagi et al., 2008). ChIP-Seq experiments show that *Sox3* binds thousands of sites in neural progenitors, many of which are associated with genes known to regulate neural development (McAninch and Thomas, 2014). Additionally, overexpression of *Sox3* maintains neural progenitors in a cycling state and blocks their differentiation (Bylund et al., 2003; Lee et al., 2012). In the zebrafish otic placode, *sox3* is initially expressed at a high level (Nikaido et al., 2007; Sun et al., 2007) and later downregulates to a discrete lower level in response to local elevation of Fgf (Padanad and Riley, 2011). The decline in *sox3* expression occurs by 12 hpf, but this is after otic fate is stably specified (Fig. 9) and is therefore not required for initiating or stabilizing otic induction. However, adjusting expression levels of *sox2* and *sox3* during early placodal development is required for proper development of sensory

and neurogenic domains that form later within the floor of the otic vesicle (Gou et al., this issue).

## Acknowledgements

This work was supported by National Institutes of Health/NIDCD grant R01-DC03806.

## References

- Adikusuma, F., Pederick, D., McAninch, D., Hughes, J., Thomas, P., 2017. Functional equivalence of the SOX2 and SOX3 transcription factors in the developing mouse brain and testes. *Genetics* 206, 1495–1503.
- Alvarez, Y., Alonso, M.T., Vendrell, V., Zelarayan, L.C., Chamero, P., Theil, T., Bösl, M.R., Kato, S., Maconochie, M., Riethmacher, D., Schimmang, T., 2003. Requirements for FGF3 and FGF10 during inner ear formation. *Development* 130, 6329–6338.
- Ambrosio, D.C., Basilico, C., Dailey, L., 1997. Synergistic activation of the fibroblast growth factor 4 enhancer by Sox2 and Oct-3 depends on protein-protein interactions facilitated by a specific spatial arrangement of factor binding sites. *Mol. Cell. Biol.* 17, 6321–6329.
- Bedell, V.M., Wang, Y., Campbell, J.M., Poshusta, T.L., Starker, C.G., Krug, R.G., Tan, W., Penheiter, S.G., Ma, A.C., Leung, A.Y.H., Fahrenkrug, S.C., Carlson, D.F., Voytas, D.F., Clark, K.J., Essner, J.J., Ekker, S.C., 2012. In vivo genome editing using a high-efficiency TALEN system. *Nature* 491, 114–118.
- Begbie, J., Brunet, J.F., Rubenstein, J.L., Graham, A., 1999. Induction of the epibranchial placodes. *Development* 126, 895–902.
- Bhat, N., Riley, B.B., 2011. Integrin- $\alpha 5$  coordinates assembly of posterior cranial placodes in zebrafish and enhances Fgf-dependent regulation of otic/epibranchial cells. *PLoS One* 6, e27778.
- Boer, B., Kopp, J., Mallanna, S., Desler, M., Chakravarthy, H., Wilder, P.J., Bernadt, C., Rizzino, A., 2007. Elevating the levels of Sox2 in embryonal carcinoma cells and embryonic stem cells inhibits the expression of Sox2: oct-3/4 target genes. *Nucleic Acids Res.* 35, 1773–1786.
- Brand, M., Heisenberg, C.P., Jiang, Y.J., Beuchle, D., Lun, K., Furutani-Seiki, M., Granato, M., Haffter, P., Hamerschmidt, M., Kane, D.A., Kelsh, R.N., Mullins, M.C., Odenthal, J., van Eeden, F.J., Nusslein-Volhard, C., 1996. Mutations in zebrafish genes affecting the formation of the boundary between midbrain and hindbrain. *Development* 123, 179–190.
- Bricaud, O., Collazo, A., 2006. The transcription factor six1 inhibits neuronal and promotes hair cell fate in the developing zebrafish (*Danio rerio*) inner ear. *J. Neurosci.* 26, 10438–10451.
- Bylund, M., Andersson, E., Novitsch, B.G., Muhr, J., 2003. Vertebrate neurogenesis is counteracted by Sox1-3 activity. *Nat. Neurosci.* 6, 1162–1168.
- Chew, J.-L., Loh, Y.-H., Zhang, W., Chen, X., Tam, W.-L., Yeap, L.-S., Li, P., Ang, Y.-S., Lim, B., Robson, P., Ng, H.-H., 2005. Reciprocal transcriptional regulation of Pou5f1 and Sox2 via the Oct4/Sox2 complex in embryonic stem cells. *Mol. Cell. Biol.* 25, 6031–6046.
- Cox, J.L., Mallanna, S.K., Luo, X., Rizzino, A., 2010. Sox2 uses multiple domains to associate with proteins present in Sox2-protein complexes. *PLoS One* 5, e15486.
- Freter, S., Muta, Y., Mak, S.-S., Rinkwitz, S., Ladher, R.K., 2008. Progressive restriction of otic fate: the role of FGF and Wnt in resolving inner ear potential. *Development* 135, 3415–3424.
- Gómez-López, S., Wiskow, O., Favaro, R., Nicolis, S.K., Price, D.J., Pollard, S.M., Smith, A., 2011. Sox2 and Pax6 maintain the proliferative and developmental potential of gliogenic neural stem cells. *In vitro. Glia* 59, 1588–1599.
- Gou, Y., Vemmaraju, S., Sweet, E.M., Kwon, H.-J., Riley, B.B., 2018. *sox2* and *sox3* play unique roles in development of hair cells and neurons in the zebrafish inner ear. *Dev. Biol.* (this issue).
- Guo, Z., Packard, A., Krolewski, R.C., Harris, M.T., Manglapus, G.L., Schwob, J.E., 2010. Expression of Pax6 and Sox2 in adult olfactory epithelium. *J. Comp. Neurol.* 518, 4395–4418.
- Hans, S., Liu, D., Westerfield, M., 2004. Pax8 and Pax2a function synergistically in otic specification, downstream of the Foxi1 and Dlx3b transcription factors. *Development* 131, 5091–5102.
- Hogan, B.L.M., Hirst, E.M.A., Horsburgh, G., Hetherington, C.M., 1988. *small eye (Sey)*: a mouse model for the genetic analysis of craniofacial abnormalities. *Development* 103, 115–119.
- Hutton, S.R., Pevny, L.H., 2011. SOX2 expression levels distinguish between neural progenitor populations of the developing dorsal telencephalon. *Dev. Biol.* 352, 40–47.
- Ikenaga, T., Urban, J.M., Gebhart, N., Hatta, K., Kawakami, K., Ono, F., 2011. Formation of the spinal network in zebrafish determined by domain-specific pax genes. *J. Comp. Neurol.* 519, 1562–1579.
- Juuri, E., Saito, K., Ahtaiainen, L., Seidel, K., Tummers, M., Hochedlinger, K., Klein, Ophir, D., Thesleff, I., Michon, F., 2012. Sox2+ stem cells contribute to all epithelial lineages of the tooth via Sfrp5+ progenitors. *Dev. Cell.* 23, 317–328.
- Kamachi, Y., Uchikawa, M., Tanouchi, A., Sekido, R., Kondoh, H., 2001. Pax6 and SOX2 form a co-DNA-binding partner complex that regulates initiation of lens development. *Genes Dev.* 15, 1272–1286.
- Kiernan, A.E., Pelling, A.L., Leung, K.K.H., Tang, A.S.P., Bell, D.M., Tease, C., Lovell-Badge, R., Steel, K.P., Cheah, K.S.E., 2005. Sox2 is required for sensory organ development in the mammalian inner ear. *Nature* 434, 1031–1035.
- Kimmel, C.B., Ballard, W.W., Kimmel, S.R., Ullmann, B., Schilling, T.F., 1995. Stages of embryonic development of the zebrafish. *Dev. Dyn.* 203, 253–310.
- Kok, Fatma O., Shin, M., Ni, C.-W., Gupta, A., Grosse, Ann, S., van Impel, A., Kirchmaier, Bettina C., Peterson-Maduro, J., Kourkoulis, G., Male, I., DeSantis, Dana F., Sheppard-Tindell, S., Ebarasi, L., Betsholtz, C., Schulte-Merker, S., Wolfe, Scot A., Lawson, Nathan D., 2015. Reverse genetic screening reveals poor correlation between morpholino-induced and mutant phenotypes in zebrafish. *Dev. Cell* 32, 97–108.
- Kondoh, H., Kamachi, Y., 2010. SOX-partner code for cell specification: regulatory target selection and underlying molecular mechanisms. *Int. J. Biochem. Cell Biol.* 42, 391–399.
- Kopp, J.L., Ormsbee, B.D., Desler, M., Rizzino, A., 2008. Small increases in the level of Sox2 trigger the differentiation of mouse embryonic stem cells. *Stem Cells* 26, 903–911.
- Léger, S., Brand, M., 2002. Fgf8 and Fgf3 are required for zebrafish ear placode induction, maintenance and inner ear patterning. *Mech. Dev.* 119, 91–108.
- Ladher, R.K., Wright, T.J., Moon, A.M., Mansour, S.L., Schoenwolf, G.C., 2005. FGF8 initiates inner ear induction in chick and mouse. *Genes Dev.* 19, 603–613.
- Lee, K., Tan, J., Morris, M.B., Rizzotti, K., Hughes, J., Cheah, P.S., Felquer, F., Liu, X., Piltz, S., Lovell-Badge, R., Thomas, P.Q., 2012. Congenital hydrocephalus and abnormal subcommissural organ development in Sox3 transgenic mice. *PLoS One* 7, e29041.
- Lee, S.A., Shen, E.L., Fiser, A., Sali, A., Guo, S., 2003. The zebrafish forkhead transcription factor Foxi1 specifies epibranchial placode-derived sensory neurons. *Development* 130, 2669–2679.
- Liu, D., Chu, H., Maves, L., Yan, Y.L., Morcos, P.A., Postlethwait, J.H., Westerfield, M., 2003. Fgf3 and Fgf8 dependent and independent transcription factors are required for otic placode specification. *Development* 130, 2213–2224.
- Lun, K., Brand, M., 1998. A series of no isthmus (noi) alleles of the zebrafish *pax2.1* gene reveals multiple signaling events in development of the midbrain-hindbrain boundary. *Development* 125, 3049–3062.
- Mackereth, M.D., Kwak, S.J., Fritz, A., Riley, B.B., 2005. Zebrafish *pax8* is required for otic placode induction and plays a redundant role with Pax2 genes in the maintenance of the otic placode. *Development* 132, 371–382.
- Mansour, S.L., Goddard, J.M., Capecchi, M.R., 1993. Mice homozygous for a targeted disruption of the proto-oncogene int-2 have developmental defects in the tail and inner ear. *Development* 117, 13–28.
- Maroon, H., Walshe, J., Mahmood, R., Kiefer, P., Dickson, C., Mason, I., 2002. Fgf3 and Fgf8 are required together for formation of the otic placode and vesicle. *Development* 129, 2099–2108.
- Martin, K., Groves, A.K., 2006. Competence of cranial ectoderm to respond to Fgf signaling suggests a two-step model of otic placode induction. *Development* 133, 877–887.
- Matsushima, D., Heavner, W., Pevny, L.H., 2011. Combinatorial regulation of optic cup progenitor cell fate by SOX2 and PAX6. *Development* 138, 443–454.
- Maulding, K., Padanad, M.S., Dong, J., Riley, B.B., 2014. Mesodermal Fgf10b cooperates with other fibroblast growth factors during induction of otic and epibranchial placodes in zebrafish. *Dev. Dyn.* 243, 1275–1285.
- McAninch, D., Thomas, P., 2014. Identification of highly conserved putative developmental enhancers bound by SOX3 in neural progenitors using ChIP-Seq. *PLoS One* 9, e113361.
- Meeker, N.D., Hutchinson, S.A., Ho, L., Trede, N.S., 2007. Method for isolation of PCR-ready genomic DNA from zebrafish tissues. *Biotechniques* 43 (610), 612, (614).
- Millimaki, B.B., Sweet, E.M., Riley, B.B., 2010. Sox2 is required for maintenance and regeneration, but not initial development, of hair cells in the zebrafish inner ear. *Dev. Biol.* 338, 262–269.
- Miyagi, S., Masui, S., Niwa, H., Saito, T., Shimazaki, T., Okano, H., Nishimoto, M., Muramatsu, M., Iwama, A., Okuda, A., 2008. Consequence of the loss of Sox2 in the developing brain of the mouse. *FEBS Lett.* 582, 2811–2815.
- Nechiporuk, A., Linbo, T., Raible, D.W., 2005. Endoderm-derived Fgf3 is necessary and sufficient for inducing neurogenesis in the epibranchial placodes in zebrafish. *Development* 132, 3717–3730.
- Nikaido, M., Shimizu, T., Hibi, M., Kikuchi, Y., Yamasu, K., 2007. Initial specification of the epibranchial placode in zebrafish embryos depends on the fibroblast growth factor signal. *Dev. Dyn.* 236, 564–571.
- Packard, A.I., Lin, B., Schwob, J.E., 2016. Sox2 and Pax6 play counteracting roles in regulating neurogenesis within the murine olfactory epithelium. *PLoS One* 11, e0155167.
- Padanad, M.S., Bhat, N., Guo, B., Riley, B.B., 2012. Conditions that influence the response to Fgf during otic placode induction. *Dev. Biol.* 364, 1–10.
- Padanad, M.S., Riley, B.B., 2011. Pax2/8 proteins coordinate sequential induction of otic and epibranchial placodes through differential regulation of foxi1, sox3 and fgf24. *Dev. Biol.* 351, 90–98.
- Park, B.-Y., Saint-Jeannet, J.-P., 2008. Hindbrain-derived Wnt and Fgf signals cooperate to specify the otic placode in *Xenopus*. *Dev. Biol.* 324, 108–121.
- Phillips, B.T., Bolding, K., Riley, B.B., 2001. Zebrafish fgf3 and fgf8 encode redundant functions required for otic placode induction. *Dev. Biol.* 235, 351–365.
- Rizzino, A., Wuebben, E.L., 2016. Sox2/Oct4: a delicately balanced partnership in pluripotent stem cells and embryogenesis. *Biochim. Et. Biophys. Acta (BBA) - Gene Regul. Mech.* 1859, 780–791.
- Robu, M.E., Larson, J.D., Nasevicius, A., Beiraghi, S., Brenner, C., Farber, S.A., Ekker, S.C., 2007. p53 activation by knockdown technologies. *PLoS Genet.* 3, e78.
- Rossi, A., Kontarakis, Z., Gerri, C., Nolte, H., Holper, S., Kruger, M., Stainier, D.Y.R., 2015. Genetic compensation induced by deleterious mutations but not gene knockdowns. *Nature* 524, 230–233.
- Schulte-Merker, S., Stainier, D.Y.R., 2014. Out with the old, in with the new: reassessing morpholino knockdowns in light of genome editing technology. *Development* 141,



- 3103–3104.
- Smith, A.N., Miller, L.-A., Radice, G., Ashery-Padan, R., Lang, R.A., 2009. Stage-dependent modes of Pax6-Sox2 epistasis regulate lens development and eye morphogenesis. *Development* 136, 2977–2985.
- Soufi, A., Garcia, Meilin, F., Jaroszewicz, A., Osman, N., Pellegrini, M., Zaret, Kenneth, S., 2015. Pioneer transcription factors target partial DNA motifs on nucleosomes to initiate reprogramming. *Cell* 161, 555–568.
- Stavridis, M.P., Lunn, J.S., Collins, B.J., Storey, K.G., 2007. A discrete period of FGF-induced Erk1/2 signalling is required for vertebrate neural specification. *Development* 134, 2889–2894.
- Steevens, A.R., Sookiasian, D.L., Glatzer, J.C., Kiernan, A.E., 2017. SOX2 is required for inner ear neurogenesis. *Sci. Rep.* 7, 4086.
- Sun, S.K., Dee, C.T., Tripathi, V.B., Rengifo, A., Hirst, C.S., Scotting, P.J., 2007. Epibranchial and otic placodes are induced by a common Fgf signal, but their subsequent development is independent. *Dev. Biol.* 303, 675–686.
- Tucker, E.S., Lehtinen, M.K., Maynard, T., Zirlinger, M., Dulac, C., Rawson, N., Pevny, L., LaMantia, A.-S., 2010. Proliferative and transcriptional identity of distinct classes of neural precursors in the mammalian olfactory epithelium. *Development* 137, 2471–2481.
- Wang, T.-W., Stromberg, G.P., Whitney, J.T., Brower, N.W., Klymkowsky, M.W., Parent, J.M., 2006. Sox3 expression identifies neural progenitors in persistent neonatal and adult mouse forebrain germinative zones. *J. Comp. Neurol.* 497, 88–100.
- Wright, T.J., Mansour, S.L., 2003. *Fgf3* and *Fgf10* are required for mouse otic placode induction. *Development* 130, 3379–3390.
- Xiao, T., Roeser, T., Staub, W., Baier, H., 2005. A GFP-based genetic screen reveals mutations that disrupt the architecture of the zebrafish retinotectal projection. *Development* 132, 2955–2967.